RIGOROUS PHOTOGRAMMETRIC PROCESSING OF HIRISE STEREO IMAGES FOR MARS TOPOGRAPHIC MAPPING

Ron Li, Ju Won Hwangbo, Yunhang Chen, and Kaichang Di

Mapping and GIS Laboratory, Department of Civil and Environmental Engineering and Geodetic Science, The Ohio State University, 470 Hitchcock Hall, 2070 Neil Avenue, Columbus, OH 43210-1275 - (li.282, hwangbo.2, chen.1256, di.2)@osu.edu

Commission IV, WG IV/7

KEY WORDS: Digital Photogrammetry, Sensor Models, Bundle Adjustment, Mars Topographic Mapping, High-resolution Imaging, Matching, Extraterrestrial Remote Sensing

ABSTRACT:

High-resolution (submeter) orbital imagers opened possibilities for Mars topographic mapping with unprecedented precision. While the typical sensor model for other Martian orbiters has been the linear array CCD, HiRISE is based on a more complicated structure involving combination of 14 separate linear array CCDs. To take full advantage of this high-resolution capability without compromising imaging geometry, we developed a rigorous photogrammetric model for HiRISE stereo image processing. Second-order polynomials are used to model the change in EO parameters over time. A coarse-to-fine hierarchical matching approach was developed and its performance is evaluated based on manually generated tie points for a test area at the Mars Exploration Rover Spirit landing site. We then performed bundle adjustment for improving image pointing data using 500 tie points selected from a set of matched interest points. Finally, we created a 1-m-resolution Digital Elevation Model (DEM) and compared the DEM with a DEM from the U.S. Geological Survey.

1. INTRODUCTION

High-precision topographic information is critical to exploration of the Martian surface. Topographic information can be derived from both orbital (satellite) and ground (lander/rover) data. The availability of HiRISE (High Resolution Imaging Science Experiment) stereo images has made great progress in high-resolution imaging and topographic and morphological information derivation for Mars surface exploration (McEwen et al., 2007). To take advantage of this new technology, we have developed a rigorous photogrammetric model for HiRISE stereo image processing, and compared our result (DEM) with that from the USGS, whose method was to pre-process the images to remove the optical distortion so that a "generic" sensor model could be used (Kirk, 2007. Our approach consists of image processing/matching and bundle adjustment. For image processing, radiometric enhancement was conducted to remove systematic noise in the raw images. Then automatic hierarchical matching was performed. Bundle adjustment aimed at removing the inconsistencies between HiRISE stereo images by adjusting their EO parameters based on the rigorous stereo model (Li et al., 2007, 2008).

2. RIGOROUS MODELING OF HIRISE STEREO DATA

2.1 HiRISE Imaging Geometry

HiRISE is a push-broom imaging sensor with 14 CCDs (10 red, 2 blue-green and 2 NIR). Each CCD consists of a block of 2048 pixels in the across-track direction and 128 pixels in the along-track direction. Ten CCDs covering the red spectrum (700 nm) are located in the middle (Figure 1, Delamere et al., 2003; McEwen et al., 2007).
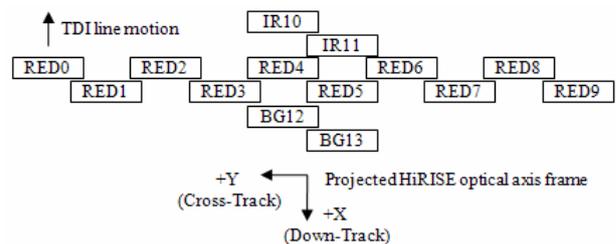
Figure 1. HiRISE CCD layout (after McEwen et al, 2007)

In the cross-track direction, average overlap width between adjacent CCDs is about 48 pixels. However, the alignment of CCDs involves small shifts and rotations with regarding to the HiRISE optical axis. After excluding overlapping pixels, HiRISE can generate images with a swath of up to 20,264 pixels (cross-track) and a 30 cm/pixel resolution at a 300 km altitude (Delamere et al., 2003; McEwen et al, 2007). At such a high resolution, the IFOV (instantaneous field-of-view) is extremely small and, as result, the ground track speed becomes very fast. To improve the signal strength of "fast-moving" objects and to increase the exposure time, Time Delay Integration (TDI) technology has been incorporated in the instrument. As the MRO (Mars Reconnaissance Orbiter) spacecraft moves above the surface of Mars, TDI integrates the signal as it passes across the CCD detector by shifting the accumulated signal into the next row (line) of the CCD at the same rate as the image moves (line rate of 13000 lines/sec = 1 line every 76 microsecond). Signals in each TDI block are transferred from line to line at ground track speed. A single pixel is formed by accumulating signals from the TDI block. HiRISE can use 8, 32, 64 or 128 TDI stages to match scene radiance to the CCD full well capacity. According to the HiRISE instrument kernel (Semenov, 2007), the observation time of a single pixel is defined as the

Ephemeris Time (ET) when the center of the TDI block is exposed.

The HiRISE instrument kernel provides the calibrated interior orientation parameters needed to calculate the pixel view direction with respect to the HiRISE frame (MRO_HIRISE_OPTICAL_AXIS). In the raw image, the row position of each pixel is related to the Ephemeris Time, which then determines the position and orientation of the HiRISE frame. The CCD ID and the column position are translated into the physical position of a pixel in the HiRISE frame. If a pixel in CCD i is located at column m, the following equations can be used to retrieve the ideal focal plane coordinates.

$$
\begin{aligned}
u &= TDI/2 - 64 - (BIN/2 - 0.5) \\
v &= (m - 0.5) \cdot BIN - 1024 \\
x &= transx_{i,0} + transx_{i,1} \cdot v + transx_{i,2} \cdot u \\
y &= transy_{i,0} + transy_{i,1} \cdot v + transy_{i,2} \cdot u \\
r &= (x^2 + y^2)^{1/2} \\
dr/r &= -0.0048509 + (r^2 \cdot 2.41312 \cdot 10^{-7}) \\
&\quad + (r^4 \cdot -1.62369 \cdot 10^{-13}) \\
xp &= x - (dr/r) \cdot x \\
yp &= y - (dr/r) \cdot y
\end{aligned}
\tag{1}
$$

where u, v = pixel position with respective to CCD center
TDI = number of TDI elements in the along-track direction (8, 32, 64 or 128)
BIN = binning mode (1, 2, 3, 4, 8, or 16)
m = pixel position in column direction
x, y = pixel position with respect to HiRISE optical axis
$transx_{i,k}$, $transy_{i,k}$ = calibration parameters ($k = 0,1,2$)
xp, yp = ideal focal plane coordinates after elimination of radial distortion

2.2 Image Pointing Data

Exterior Orientation (EO) parameters, which are the positions of the camera perspective center and pointing angles at a specific time, are provided in SPICE kernels. The EO parameters of each image line can be retrieved by interpolating the spacecraft's trajectory and pointing vectors. Previous research has shown that the change in EO parameters over short trajectories can be well modeled using polynomials (Yoon and Shan 2005; Li et al., 2007, 2008). In this research, second-order polynomials are used to model this change

$$
\begin{aligned}
X^c_i &= a_0 + a_1 t + a_2 t^2 & \omega^c_i &= d_0 + d_1 t + d_2 t^2 \\
Y^c_i &= b_0 + b_1 t + b_2 t^2 & \varphi^c_i &= e_0 + e_1 t + e_2 t^2 \\
Z^c_i &= c_0 + c_1 t + c_2 t^2 & \kappa^c_i &= f_0 + f_1 t + f_2 t^2
\end{aligned}
\tag{2}
$$

where X^c_i, Y^c_i, Z^c_i = position of the perspective center of the sensor of the ith line (time t)
ω_i, φ_i, κ_i = pointing angles of the ith line
a_0, ..., f_2 = polynomial coefficients
t = time-dependent image line index number

Modeled this way, EO parameters can be adjusted by refining the 36 polynomial coefficients of the stereo pair. Since all 14 CCDs are fixed to the HiRISE frame, they share the same perspective center and focal plane. Therefore, changes in the EO parameters of all 14 CCDs yield one set of polynomial coefficients. This critical characteristic significantly reduces the complexity of the bundle adjustment of HiRISE stereo images. Images simultaneously generated by multiple CCD arrays can

be processed together under a uniform rigorous sensor model in the bundle adjustment instead of being processed strip by strip.

To apply the above strategy, one reference CCD strip must be assigned; this strip can be arbitrarily chosen. Then the offsets between other CCD strips and the reference strip are calculated by comparing their EO data line by line. The line (row) index of the EO polynomials of the reference strip starts from zero. For the other non-reference strips, it starts from the offsets. The initial value of the EO polynomial coefficients can be estimated by least-squares fitting of the line-by-line telemetry EO data.

Small motions of the spacecraft around its nominal pointing, called jitter, will distort the images. This problem was originally identified in the Mars Orbiter Camera (MOC) images, but was found to be more severe for HiRISE because of HiRISE's higher resolution (Kirk et al., 2007). High-frequency jitter can be filtered out by subtracting the best-fitting polynomial from the original telemetry HiRISE pointing angle data. For the 80,000 line image of Gusev Crater that was used in this study, Figure 2 shows the extracted jitter on ω, φ, κ with the horizontal axis being the image row index and the vertical axis being the jitter magnitude in arc-seconds. An analysis of the extracted residuals in the spectral domain does not show any significant frequency. Therefore, it would be very difficult to incorporate this "jitter" into a mathematical model.
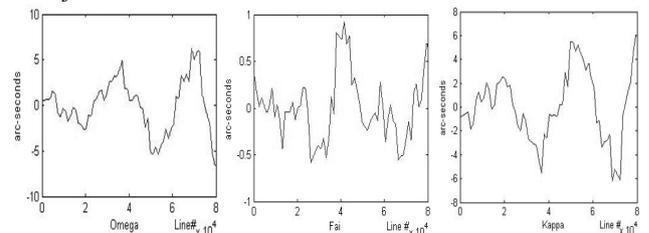
Figure 2. Residuals after subtracting best fitting polynomial from original telemetry EO data

Topographic effect of orbital jitter needs to be evaluated for topographic capability analysis of HiRISE camera. For evaluation, a single CCD pixel was projected onto the Martian surface using telemetry EO data under the assumption that Mars is a sphere with its radius derived from the nearest MOLA point. The projected footprint was compared with another projected footprint using EO parameters adopted using third-order polynomials under the same spherical assumption. A maximum difference of 2 meters, corresponding to 7 pixels on image, was detected from the comparison in a 20-kilometer track at the landing site of Mars Exploration Rover (Spirit). Further investigation on jitter will be performed so that its effects can be removed or reduced when mapping large areas.

3. PHOTOGRAMMETRIC PROCESSING OF HIRISE STEREO IMAGES

3.1 Image Matching and Tie Point Generation

We have developed a coarse-to-fine hierarchical stereo matching process (Figure 3). Raw HiRISE images contain systematic noise such as offset in the image data numbers (DN), dark current, and column-to-column gain variations (Becker, 2007). In HiRISE EDR (Experiment Data Record) data sets, the image acquired by each CCD strip (14 in total) is stored as two sub-image strips, each of which is 1024 pixels wide. Brightness values of the two sub-image strips may be inconsistent. We adjusted brightness values and then combined them together into one seamless image with a 2048-pixel wide swath. Afterwards, we removed any systematic strip noise. Then, an

image pyramid was constructed consisting of five levels. Starting with the original image, each subsequent level was created by sub-sampling the previous level's image smoothed by a Gaussian filter. Interest points were generated by Förstner operator (Förstner, 1986) at every image scale.
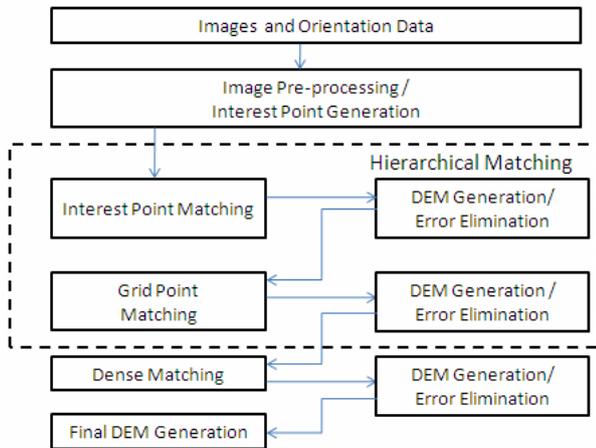
Figure 3. Workflow of the hierarchical stereo matching process

Matching started with the images of lowest resolution; results were then transferred to the next higher level, with more interest points being extracted and matched. The images, interest points and orientation parameters were used as input for the stereo matching process. At the lowest level, geographic locations of interest points were estimated by assuming a flat terrain. This enabled automatic pairing of interest points in stereo images. The search radius was confined to the neighborhood of the corresponding interest points, and matched points were selected based on correlation coefficient values.

Automatic error detection is performed at each level by eliminating outliers based on elevation distribution of neighboring points. For each point, a small local DEM surface was constructed from the matched points and modeled as a flat terrain (may be improved to a plane). Then the standard deviation of the plane estimation, σ, was calculated. If the residual of a point exceeded 2σ, it was regarded as an error and eliminated.

At subsequent levels, points from the previous level were matched again to achieve higher matching precision. A TIN (Triangulated Irregular Network) surface of parallax differences was generated from these matched points using the Delaunay triangulation method. This TIN was used to estimate the corresponding tie points. To improve matching performance for points located around the boundary of each CCD, HiRISE imaging geometry was fully utilized. Instead of mosaicking images from separate CCDs, we loosely stitched together the TIN surface based on the best-fitting alignment derived from interest point matching between adjacent CCDs.

After matching the interest points generated from the highest-resolution images, 10-pixel grid points were defined to form a basis for further matching. To generate a 1-m-resolution DEM of the terrain, 3-pixel grid points were matched. For sub-meter level DEM, dense matching was performed for every pixel in the images of highest-resolution. Evenly distributed tie points between the stereo images were selected from the set of matched interest points to be used in the subsequent bundle adjustment. The final DEM was generated after bundle adjustment and elimination of matching errors.

3.2 Matching performance evaluation

We tested this process using a stereo pair of HiRISE images that cover the Columbia Hills area of the Spirit rover landing site (TRA_001513_1655 and TRA_001777_1650). The TRA_001513 image was obtained on November 22, 2006. It is centered at 14.6 °S latitude, 175.5°E longitude. It has 27.1 cm/pixel resolution and 80,000 rows. The TRA_001777 image was taken on December 12, 2006. It has a resolution of 26.3 cm/pixel and 40,000 rows. Its extent is entirely covered by TRA_001513. The two images have a convergence angle of 19.8 degrees.

Level	Image Scale	Point Type	Residuals (pixel)		
			Mean	Standard Deviation	Maximum
1	1/16	Interest	0.26	0.55	1.41
2	1/8	Interest	0.19	0.53	2
3	1/4	Interest	0.13	0.33	1
4	1/2	Interest	0.18	0.47	1.41
5	1	Interest	0.19	0.39	1
6	1	10-pixel grid	0.06	0.24	1

Table 1. Matching residuals at intermediate levels

A quantitative evaluation of matched points was conducted for the hierarchical matching results. At each intermediate level, 16 points were randomly selected throughout the entire study area. The automatically generated matching results were compared with manually matched points. Table 1 shows the results of this evaluation of matching accuracy. The highest mean residual was found at the first level. However, this mean was still less than 1 pixel, with maximum residual being 1.41 pixels. The largest error, 2 pixels, was found at the second level. Since interest points for levels 1 through 4 were projected onto higher resolution images and adjusted by re-matching, the errors from the previous levels were not propagated into subsequent levels. While the mean residuals did not necessarily decrease over the hierarchical process, they did remain at a reasonably low level providing accurate-enough estimates of parallax differences for use at the next level.

At the final level, matching results of 3-pixel grid points were evaluated based on five test regions with different terrain types. Region 1 is a relatively flat area at the Spirit rover landing center. Region 2 is crater northeast side of Bonneville crater. Region 3 is the summit of Husband Hill. Region 4 is the Inner Basin area, located on the south side of the summit. Region 5 is Home Plate.
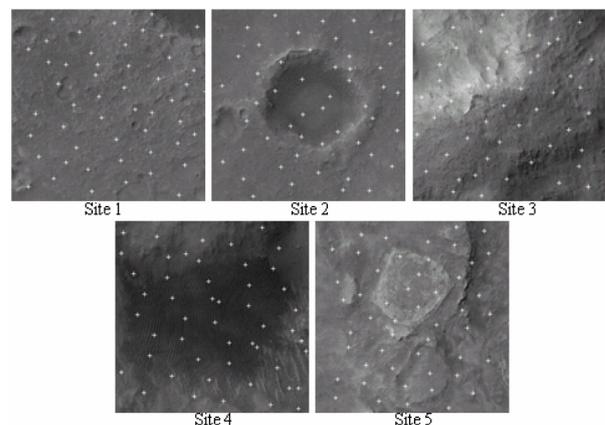
Figure 4. Distribution of check points at five test regions

Region ID	Terrain Type	Number of Points	Residuals (pixel)		
			Mean	Standard Deviation	Maximum
1	Flat	50	0.06	0.24	1
2	Crater	50	0.04	0.20	1
3	Summit	50	0.10	0.3	1
4	Dune	50	0.09	0.30	1.41
5	Flat/Ridge	50	0.11	0.33	1.41

Table 2. Matching residuals at level 7 for five test regions

For each region, 50 check points were randomly selected to verify the quality of matching results with manually generated tie points. Region 2 (crater) produced the smallest mean residuals, though only slightly lower than Region 1 (flat). Both areas contain a lot of small rocks that provide distinctive point features beneficial to matching. Region 3 includes rather smooth texture especially in the north side, while Region 4 mainly consists of a striped pattern caused by dunes. The Home Plate area (Region 5) gave the largest mean residual, which can be explained by its relative lack of detailed texture. The performance of the automatic matching varied based on the type of terrain. However, the five test regions showed consistently low residuals, averaging less than 0.11 pixel, with a maximum residual of less than 1.41 pixels.

3.3 Bundle Adjustment of HiRISE Stereo Images

Bundle adjustment aims at removing the inconsistencies between HiRISE stereo images by adjusting their EO parameters through the tie points. In our study, the initial EO parameters were retrieved from the SPICE kernel and stored line by line. The tie points were selected automatically from the matched interest points on stereo images to make sure they were evenly distributed. These tie points were then included in the bundle adjustment as measurements after the interior orientation procedure. A total of 500 tie points were selected from matched interest points for the HiRISE stereo pair in the Columbia Hill area.

In forming of the observation equations for bundle adjustment, image tie points were related to the corresponding ground coordinates and EO parameters via the collinearity equations

$$x_i + f\frac{a_{11}(X_i-X^c)+a_{12}(Y_i-Y^c)+a_{13}(Z_i-Z^c)}{a_{31}(X_i-X^c)+a_{32}(Y_i-Y^c)+a_{33}(Z_i-Z^c)}=0 \quad (3)$$

$$y_i + f\frac{a_{21}(X_i-X^c)+a_{22}(Y_i-Y^c)+a_{23}(Z_i-Z^c)}{a_{31}(X_i-X^c)+a_{32}(Y_i-Y^c)+a_{33}(Z_i-Z^c)}=0$$

where x_i = along-track coordinate of the detector on the focal plane of the ith point which can be calculated using Equation 1
y_i = corresponding cross-track image coordinate of the ith point
X_i, Y_i, Z_i = ground coordinates of the ith point
X^c, Y^c, Z^c = position of the perspective center of the sensor
$a_{11},\ldots,a_{33}$ = elements of the rotation matrix formed by the sensor pointing angles
f = focal length of the sensor

To improve the stability of the adjustment computation, telemetry data were treated as pseudo observations and were combined with linearized collinearity equations in the bundle adjustment system. The initial values of the EO polynomial coefficients were from the least-squares fitting of the telemetry EO data before bundle adjustment. The initial ground positions of tie points were obtained through a space intersection using telemetry EO data.

After bundle adjustment, the refined EO parameters were compared with those obtained from telemetry data. Figure 5 presents their differences in graphic format. The horizontal axis of Figure 5 is the image row index and the vertical axis is the difference. The BA procedure modified the camera perspective center and orientation by a maximum of close to 2 meters and the pointing angles by less than 15 arc seconds.
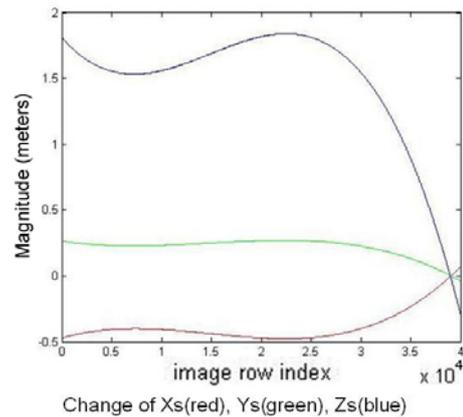
(a) Differences in camera center positions
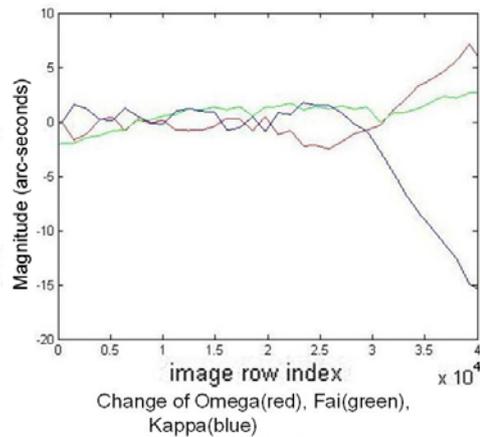
(b) Differences in sensor orientations

Figure 5. Differences between telemetry-based and refined EO parameters

Unlike the situation on Earth, no absolute ground truth is available on the Martian surface. Therefore, the performance of the bundle adjustment was evaluated in terms of back-projection residuals in the image space. Besides the tie points, a comparable number of evenly distributed check points that are matched interest points and not used in the bundle adjustment were also selected for evaluation. The differences between the measured image points and the corresponding back-projected image points represent the inconsistencies between HiRISE stereo images. Table 2 shows the corresponding statistics of the back-projection residuals on the images covering a part of Columbia Hills before and after bundle adjustment.

Status	Before BA	After BA
Mean (pixel)	1.9	0.0
Maximum (pixel)	9.2	2.6
Standard deviation (pixel)	4.4	0.85
Number of points	500 check points	

Table 3. Statistics on back-projection residuals at Columbia Hills

4. TOPOGRAPHIC MAPPING AT MER LANDING SITES

4.1 DEM Generation
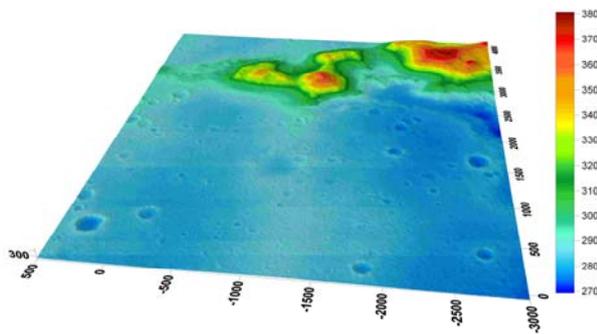
Figure 6. 3-D surface map of the area of Spirit traverse

We used 644,609 interest points and 1,556,677 grid points to perform 3-D stereo intersection of ground points based on the bundle-adjusted EO parameters. Ordinary Kriging with a spherical semi-variogram model was used to generate a 1-m-resolution DEM of the area covering the entire traverse of Spirit. Figure 6 shows the resulting 3-D surface.

4.2 DEM Comparison

To validate the quality of our DEM, we performed a comparison with a DEM generated by USGS using the same data. The comparison was done both in horizontal and in vertical directions. The two DEMs were registered through a 2-D similarity transformation based on six manually identified corresponding points. The root mean square error of these points after the transformation is 0.9 m. After horizontal registration, a vertical registration was done by a shift and a rotation in such a way that the average of the vertical differences was zero. Grid-to-grid vertical differences were then calculated. The result indicates that most areas have differences less than 1 meter (Figure 7). The standard deviation of all grid differences between those DEMs is 0.63 meter which corresponds to 2 pixels on the image.
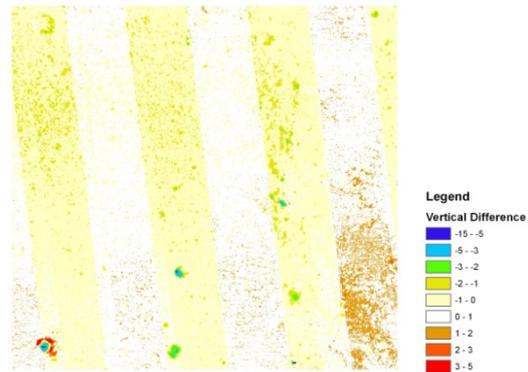
Figure 7. Vertical difference between OSU DEM and USGS DEM

There are a few features with large differences of a few meters. The most significant one is a small crater in the south west corner of the DEM. Further investigations will be performed to figure out the causes of the large differences. The strip artifact, though smaller than 1 meter in elevation, will also be investigated. Orthophoto will be generated using the validated DEM, the original HiRISE imagery and the bundle-adjusted EO parameters.

5. CONCLUSIONS

In this paper, we presented a rigorous photogrammetric processing approach for automatic DEM generation from HiRISE images. Our approach employs a coarse-to-fine hierarchical matching method that can provide dense and reliable tie points for both DEM generation and bundle adjustment. First, interest points were matched up to the level of original image scale. Then grid points were defined and matched, also moving from coarse to fine grid scale. For quality control, an automatic error detection algorithm was incorporated at each hierarchical level. We evaluated the performance of our matching results for a test area covering the entire Spirit traverse. At intermediate levels, the mean residual remained lower than 0.3 pixel, providing a TIN surface of parallax difference to provide estimation for dense grid points matching. At the final level, with 3-pixel grid spacing, the mean residual was less than 0.11 pixel. We performed a bundle adjustment to reduce the inconsistencies between HiRISE stereo images. In the bundle adjustment, second-order polynomials were used to model the change of EO parameters over time. We chose 500 tie points from the matched interest points for bundle adjustment. The performance was evaluated based on back-projection residuals of the independent check points. The mean residual was reduced from 1.9 pixels to zero. Also, the standard deviation of the residuals decreased from 4.4 pixels to 0.85 pixel. We created a DEM of the area covering the Spirit rover traverse, which was compared with a DEM generated by the USGS.

REFERENCES

Becker, K., et al., 2007. Processing HiRISE images using ISIS 3, *Lunar and Planetary Science XXXVIII*, Houston, TX, #1779.

Delamere, A. W., et al., 2003. MRO High Resolution Imaging Science Experiment (HiRISE): Instrument development, *Sixth International Conference on Mars*. Houston, TX, #3260.

Förstner, W., 1986. A feature based correspondence algorithm for image matching, *Intl. Arch. Photogrammetry and Remote Sensing*, 26(3), pp. 150–166.

Kirk, R., et al., 2007. Ultrahigh resolution topographic mapping of Mars with HiRISE stereo images: methods and first results. *Seventh International Conference on Mars*, Pasadena, CA, #3391.

Li, R., et al., 2007. Integration of Orbital and Ground Images for Enhanced Topographic Mapping in Mars Landed Missions, *Annual NASA Science Technology Conference*, College Park, MD, June 19-21. (unpaginated CD-ROM).

Li, R., et al, 2008. Rigorous Photogrammetric Processing Of Hirise Stereo Images And Topographic Mapping At Mars Exploration Rover Landing Sites, *39th Lunar and Planetary Science Conference*, League, TX, #1864.

McEwen, A., et al., 2007. Mars Reconnaissance Orbiter's High Resolution Imaging Science Experiment (HiRISE). *Journal of Geophysical Research*, 112 (E05S02).

Semenov, B., 2007. HIRISE instrument kernel, ver. 1.0. NAIF/JPL. ftp://naif.jpl.nasa.gov/pub/naif/MRO/kernels/ik/ mro_hirise_v10.ti (last accessed 11 April 2008).

Shan, J., et al., 2005. Photogrammetric analysis of the Mars Global Surveyor mapping data, *PE & RS*, 71(1), pp. 97–108.

Yoon, J., and J. Shan, 2005. Combined adjustment of MOC stereo imagery and MOLA altimetry data. *PE & RS*, 71(10), pp. 1179–1186